Article

Not peer-reviewed version

Ramsey and Turán Structures Generated by Tessellations

Artem Gilevich , Shraga Shoval , Edward Bormashenko *

Posted Date: 4 June 2026

doi: 10.20944/preprints202606.0392.v1

Keywords: tessellation; graph theory; Ramsey graph; Turán numbers

 doi:10.20944/preprints202606.0392.v1

Article

Ramsey and Turán Structures Generated by Tessellations

Artem Gilevich [1], Shraga Shoval [2] and Edward Bormashenko [1,*]

[1] Department of Chemical Engineering, Biotechnology and Materials, Engineering Faculty, Ariel University, Ariel, 407000, Israel

[2] Department of Industrial Engineering and Management, Engineering Faculty, Ariel University, P.O. Box 3, Ariel 407000, Israel

* Correspondence: edward@ariel.ac.il

Abstract

Plane tessellations naturally generate local combinatorial invariants such as vertex degree and vertex type, which encode essential geometric and topological information. In the present work, these invariants are used to construct complete bicolored graphs whose edge coloring is induced intrinsically by the equality or inequality of local tessellation properties. Two classes of structured Ramsey graphs are introduced: vertex-degree graphs and vertex-type graphs. Unlike classical Ramsey colorings, the proposed colorings are not arbitrary but arise from equivalence relations generated by local geometric invariants. Consequently, the resulting graphs possess a partition-generated or semi-transitive structure in which one color forms disjoint complete cliques corresponding to equivalence classes, while the complementary color connects distinct classes. Within this framework, a sharp Ramsey-type theorem is established: every such graph on five vertices necessarily contains a monochromatic triangle. The combinatorial core of the theorem reduces to the statement that among five values either three coincide or three are pairwise distinct. Turán numbers for the introduced structured colorings are calculated and shown to possess a characteristic asymmetry that is absent in classical extremal graph theory. The relationship between geometric symmetries of tessellations and automorphism groups of the associated Ramsey graphs is analyzed, demonstrating that tessellation symmetries induce graph automorphisms, while additional purely combinatorial symmetries may emerge from degree degeneracies. The results establish a direct connection between tessellation geometry, equivalence relations, Ramsey theory, and extremal graph theory.

Keywords: tessellation; graph theory; Ramsey graph; Turán numbers

MSC: 05C15; 05B45; 05D10

1. Introduction

Plane tessellations constitute a classical object of geometry, combining local combinatorial structure with global symmetry. A tessellation encodes extensive information through simple local invariants such as vertex degree (valency) and vertex type, which reflects how polygons meet at a point. These local characteristics are preserved under geometric symmetries and therefore serve as natural invariants in the study of periodic and non-periodic tilings [1–3].

In parallel, Ramsey theory studies unavoidable patterns in sufficiently large structures. A central result asserts that any sufficiently large edge-coloured complete graph necessarily contains monochromatic subgraphs of prescribed type [4–6]. Closely related extremal problems are addressed within Turán theory, which studies the maximal number of edges avoiding prescribed subgraphs [7–9]. Classical Ramsey theory deals with arbitrary colourings; however, in many natural settings, colourings are not arbitrary but generated by intrinsic structures. Understanding how such

 doi:10.20944/preprints202606.0392.v1

structured colourings influence Ramsey-type phenomena remains an important and largely unexplored direction.

In this work, we introduce a new class of structured bicolored graphs generated by tessellations, which we call vertex-degree Ramsey graphs (VDG) and vertex-type Ramsey graphs (VTG). In these constructions, the colouring is not imposed externally but arises from the equality or inequality of local geometric invariants. Specifically, edges are coloured according to whether two vertices share the same degree or the same vertex type (defined by the specific arrangement and sides of polygons meeting at a vertex). This leads to a highly constrained class of colourings, which we term semi-transitive or partition-generated graphs.

The key structural feature of these graphs is that one colour corresponds to an equivalence relation and therefore forms a disjoint union of complete cliques, while the complementary colour connects different equivalence classes. Thus, the entire graph is completely determined by a partition of the vertex set. This sharply contrasts with arbitrary Ramsey colourings and places the problem in a fundamentally different combinatorial regime [6,9–11]. Within this framework, we establish a sharp Ramsey-type result: every vertex-degree or vertex-type graph on five vertices necessarily contains a monochromatic triangle. Remarkably, this result reduces to a purely combinatorial statement about integers: among five values, either three coincide or three are pairwise distinct. The tessellation provides a geometric realization of this combinatorial principle.

Combinatorial properties of tessellations were addressed recently [12]. In particular, combinatorial properties of the Voronoi tessellations were reported [13]. Voronoi tessellations represent a convenient and important mathematical structure for the suggested Ramsey analysis [14–22]. Voronoi diagrams provide a natural framework for studying statistical tessellation-generated Ramsey structures and enable the investigation of equivalence-based and non-transitive graph topologies arising in disordered geometric systems.

A second central focus of the paper is the calculation of Turán numbers for semi-transitive graphs [23–25]. Unlike classical extremal graph theory, where a single extremal number is considered, the present setting naturally leads to a pair of extremal quantities corresponding to the two colours. We show that these extrema are asymmetric and cannot be realized simultaneously, revealing a new structural feature of partition-generated colorings.

We further analyze the relationship between geometric symmetry of tessellations and combinatorial symmetry of the associated Ramsey graphs. We demonstrate that the passage from tessellations to vertex-degree graphs acts as a projection: geometric symmetries induce graph automorphisms, but additional purely combinatorial symmetries may emerge due to degeneracy of degree classes. This leads to the general relation $\Phi(H_X) \subseteq Aut(G_X)$, where G_X is a graph on X vertexes set, which is strict in typical cases [10,23–25].

Finally, we extend the construction from vertex degree to vertex types, showing that the same Ramsey phenomenon persists when the colouring is induced by equality of vertex type. This demonstrates that the observed behaviour is not specific to the degree, but reflects a broader principle: Ramsey-type structures naturally emerge from equivalence relations generated by local invariants of tessellations.

The results presented in this paper establish a direct bridge between geometry, combinatorics, and extremal graph theory. They show that tessellations provide a natural source of structured Ramsey graphs in which combinatorial inevitability arises not from randomness or size alone, but from intrinsic geometric constraints.

2. Mathematical Foundations and Definitions

2.1. Vertex-Degree Ramsey Graphs Generated by Tessellations

We start with an arbitrary plane tessellation T. Let $V(T)$ be set of its vertices. For every vertex $v \in V(T)$ we introduce its degree or valency, namely the number of edges of the tessellation meeting at v, denoted $d(v)$. Now we introduce the notion of the vertex-degree graph abbreviated VDG.

 doi:10.20944/preprints202606.0392.v1

Definition 1. Definition of the vertex-degree graph (VDG).

Choose a finite set of vertices $X = \{v_1, \dots, v_n\} \subset V(T)$ from a given tessellation T. We construct the complete graph K_n on these vertices, and color each edge $\{v_i, v_j\}$ as follows:

$$col_{ij}(v_i, v_j) = \begin{Bmatrix} \text{green}, & \text{if } d(v_i) = d(v_j) \\ \text{red}, & \text{if } d(v_i) \neq d(v_j) \end{Bmatrix}, \quad (1)$$

where col_{ij} is the coloring function. Thus, the tessellation generates a complete bicolored graph $G_X = \{X, E, col\}$, where $E = \{\{v_i, v_j\}: i \neq j\}$, and *col* is the above coloring rule.

Thus, a complete bicolored, vertex-degree Ramsey graph (VDG) emerges. This is not an arbitrary 2-coloring. It is generated by equality/inequality of a numerical invariant, namely vertex degree. Therefore, the coloring of VDG has an internal structure. Define a relation on vertices by

$$v_i \sim v_j \leftrightarrow d(v_i) = d(v_j). \quad (2)$$

The relation defined by Eq. 2 is an equivalence relation. Hence the green edges join vertices belonging to the same equivalence class, while red edges join vertices from different classes. So, the graph has the following structure: the green subgraph is a disjoint union of complete cliques, the red edges connect vertices belonging to different green cliques. This is what may be called a semi-transitive or partition-generated Ramsey graph. Now we introduce the notion of degree classes.

Definition 2. Degree classes

The equivalence classes induced by equality of vertex degree are called the degree classes of X. Then, green cliques are exactly the complete subgraphs generated by individual degree classes. Thus, structural Theorem 1 immediately emerges.

Theorem 1.

Every vertex-degree Ramsey graph of a tessellation is completely determined by the partition of the chosen vertices into degree classes.

Proof

The color of an edge of a VDG depends solely on whether its endpoints belong to the same or different degree classes. Hence once the partition into equal-degree classes is known, every edge color is fixed. So, the graph is a partition graph in the strongest possible sense.

The relation $d(v_i) = d(v_j)$ establishing the green color of the edge linking vertices i and j is transitive, thus if vertices i and j are connected with a green link, and vertices j and k are connected with a green link, necessarily vertices i and k are also connected with an green link. However, the relation $d(v_i) \neq d(v_j)$ establishing the red color of the edge linking vertices i and j is not transitive. If vertices i and j are connected with a red link, and vertices j and k are connected with a red link, it is possible that vertices i and k are connected with a red link, and it is also possible that they are connected with a green link. Thus, VDG is not a usual Ramsey graph; is it the semi-transitive Ramsey graph. A semi-transitive Ramsey graph with five vertices necessarily contains at least one monochromatic triangle, as demonstrated in the following theorem.

Theorem 2

Let $X = \{v_1, \dots, v_n\}$ be any set of five vertices chosen from a plane tessellation, and let G_X be the complete bicolored graph defined by $col_{ij}(v_i, v_j) = \begin{Bmatrix} \text{green}, & \text{if } d(v_i) = d(v_j) \\ \text{red}, & \text{if } d(v_i) \neq d(v_j) \end{Bmatrix}$. Then G_X contains a monochromatic triangle.

Proof

Define on set X the equivalence relation $v_i \sim v_j \leftrightarrow d(v_i) = d(v_j)$. Let the equivalence classes of this relation be the degree classes $X_1, X_2, \dots, X_m$; $\sum_{i=1}^{m} X_i = 5$. By construction: if two vertices belong to the same class X_r, the edge joining them is green; if two vertices belong to different classes, the edge joining them is red. We now distinguish between two cases:

Case 1. One degree class contains at least three vertices.

Assume that for some r, $X_r \geq 3$. Choose three distinct vertices $a, b, c \in X_r$. Since all three belong to the same degree class, we have $d(a) = d(b) = d(c)$. Hence the three edges $\{a, b\}$, $\{b, c\}$ and $\{a, c\}$ are green, therefore *a*, *b*, *c* forms an green triangle.

Case 2. Every degree class contains at most two vertices

 doi:10.20944/preprints202606.0392.v1

Assume now that $X_r \leq 2$ for all r. Since the total number of vertices is 5, it is impossible to cover all five vertices with only one or two classes of size at most 2. Therefore, there must be at least three distinct degree classes. This allows us to choose vertices $a \in X_r$, $b \in X_s$, $c \in X_t$ from three different classes X_r, X_s, X_t. Because these vertices belong to different degree classes, their degrees are pairwise different: $d(a) \neq d(b) \neq d(c)$. Hence all three edges $\{a, b\}$, $\{b, c\}$ and $\{a, c\}$ are red, and therefore a, b, c form a red triangle. In both cases, G_X contains a monochromatic triangle. This proves the theorem.

Simply speaking: The coloring is induced by the equivalence relation $v_i \sim v_j \leftrightarrow d(v_i) = d(v_j)$, so the chosen vertices are partitioned into degree classes. If one degree class contains at least three vertices, these three vertices form the red triangle. If every degree class has size of at most two, then five vertices must occupy at least three distinct degree classes; choosing one vertex from each of the three classes yields a red triangle, since vertices from different classes are joined by red edges. Hence, a monochromatic triangle always exists. In other words, every partition-generated 2-coloring of K_5 has a monochromatic triangle. Using the terminology of tessellations, we state that in any set of five vertices of a tessellation, one necessarily finds either a triple of equal valency or a triple of mutually different valencies. The generalization of Theorem 2 is straightforward. Since the coloring depends only on the degree of the vertices, the whole construction reduces to a statement about integers. Given five integers $\{d_1, \dots, d_5\}$ either: three of them are equal, or three of them are pairwise distinct.

This is exactly the combinatorial core of Theorem 2. The tessellation supplies the geometric meaning of the integers. The extension for regular tessellations is trivial.

In a regular tessellation all vertices have the same degree, so every edge is red. The degree-Ramsey graph is therefore a complete red clique.

2.2. Calculation of the Turán Numbers for the Semi-Transitive Graphs

Now, we calculate the Turán numbers for the semi-transitive graphs [26]. Consider a semi-transitive graph with n vertices. Let the degree classes have sizes:

$$s_1, s_2, \dots, s_m;\ \sum_{r=1}^{m} s_r = 1. \tag{3}$$

Green edges occur inside degree classes:

$$E_{\text{green}} = \sum_{r=1}^{m} \binom{s_r}{2}. \tag{4}$$

Red edges occur between different degree classes:

$$E_{\text{red}} = \sum_{r<t} s_r s_t. \tag{5}$$

A green triangle appears exactly if and only if at least one degree class has a size of at least three. Therefore, to avoid green triangles, all degree classes must have size of at most 2. The maximal number of green edges is then obtained by splitting the vertices into pairs: $2 + 2 + \cdots + 2$, and possibly one remaining vertex. Hence:

$$ex_{\text{green}}(n, K_3) = \left[\frac{n}{2}\right] \tag{6}$$

A red triangle appears exactly when there are at least three distinct degree classes. Therefore, to avoid red triangles, the partition may contain at most two degree classes. The number of red edges is then maximized by splitting the vertices into two classes as evenly as possible, namely: $\left[\frac{n}{2}\right], \left[\frac{n}{2}\right]$. Thus, we calculate:

$$ex_{\text{green}} = (n, K_3) = \left[\frac{n}{2}\right] \times \left[\frac{n}{2}\right] = \left[\frac{n^2}{4}\right]. \tag{7}$$

For five vertices: $ex_{\text{green}}(5, K_3) = 2$ realized by the partition 2+2+1, while $ex_{\text{red}} = (5, K_3) = 6$, realized by partition $3 + 2$. It should be emphasized that these two extrema are not realized simultaneously. The partition 2+2+1 avoids green triangles but it already contains a red triangle. The partition $3 + 2$ avoids red triangles but contains an green triangle. This asymmetry is the distinctive Mantel–Turán feature of semi-transitive VDGs. Finally, the Turán numbers for semi-transitive graphs are given by Eq. 6 and Eq. 7.

 doi:10.20944/preprints202606.0392.v1

2.3. Symmetry of the Tessellation and Symmetry of the Vertex-Degree Ramsey Graph

Let T be a plane tessellation, and let $\mathfrak{H} = \{h_1, \dots, h_m\}$ be its symmetry group, i.e. the group of all isometries of the plane mapping T onto itself. Let $X = \{v_1, \dots, v_n\} \subset V(T)$ be a finite set of vertices, and let G_X be the corresponding vertex-degree Ramsey graph. Note that every symmetry $h \in \mathfrak{H}$ preserves the degree of a vertex:

$$d(h(v)) = d(v), v \in V(T), \quad (8)$$

Indeed, an isometry that maps the tessellation onto itself preserves the local incidence structure of edges meeting at every vertex, and therefore preserves valency. Hence, if $v_i, v_j \in X$, then:

$$d(v_i) = d(v_j) \leftrightarrow d(h(v_i)) = d\left(h(v_j)\right). \quad (9)$$

Therefore, the color of the edge $\{v_i, v_j\}$ is the same as the color of the edge $\{h(v_i,), h(v_j)\}$. It should be emphasized that the symmetry group of the tessellation does not automatically pass to the graph in full, but is restricted to the subgroup that stabilizes the set X. More precisely, if we define the stabilizer $\mathfrak{H}_X = \{h \in \mathfrak{H}: h(X) = X\}$, then every element of $\mathfrak{H}_X$ induces a color-preserving automorphism of G_X. The stabilizer $\mathfrak{H}_X$ consists of all symmetries of the tessellation that map the chosen vertex set X onto itself. Therefore, there is a natural group homomorphism $\Phi: \mathfrak{H}_X \to Aut(G_X)$. In particular, symmetry-equivalent vertices always belong to the same degree class, so degree classes are unions of symmetry orbits. For vertex-transitive tessellations all vertices have the same degree, and the corresponding graph G_X is a complete green clique.

It is not true in general that $Aut(G_X) = H_X$, rather $\Phi(H_X) \subseteq Aut(G_X)$. The graph retains only information regarding vertex degrees, rather than the full geometry of the tessellation. So, the graph may have "extra" automorphisms obtained by permuting vertices within the same degree class, even when these permutations do not come from geometric symmetries of the tessellation. Thus, the passage from the tessellation to the vertex-degree Ramsey graph may be viewed as a projection from geometric symmetry to combinatorial symmetry, in which part of the geometric information is lost while new purely combinatorial symmetries may emerge.

This is well-exemplified with the seminal Cairo tiling depicted in Figure 1.

Example 1. Symmetry and VDG of Cairo tiling

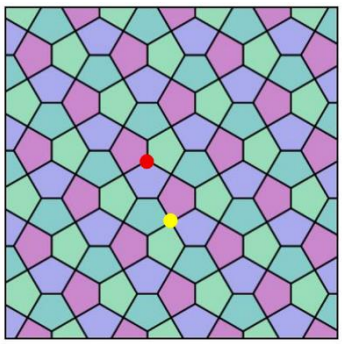

Figure 1. Cairo tiling. The Cairo tiling is a periodic plane tessellation by congruent convex pentagons, widely known from the paving patterns of streets in Cairo. It belongs to the class of monohedral pentagonal tilings and possesses wallpaper symmetry group *p4g*. Red point corresponds to the 3-valency vertex, yellow – to the 4-valency vertex.

The Cairo tiling is a standard periodic pentagonal tiling [27–30]; in the dual-to-snub-square form it has wallpaper symmetry group *p4g*, and its vertices are of two valencies, 3 and 4, i.e. $V(T) = C_3 \cup C_4$, where vertices in C_3 have degree 3 and vertices in C_4 have degree 4. Because every symmetry of the tessellation preserves valency, every symmetry sends C_3 to C_3, and C_4 to C_4. Thus, the geometric symmetry group acts on the two-degree classes, but it is constrained by the actual embedding of the vertices in the plane. Now choose a finite subset $X \subset V(T)$ containing, say, three vertices from C_3 and two vertices from C_4 and choose them generically, so that no nontrivial symmetry of the Cairo tiling preserves X as a set. Then the stabilizer $\mathfrak{H}_X = \{h \in \mathfrak{H}: h(X) = X\}$ may be

 doi:10.20944/preprints202606.0392.v1

trivial. In contrast, the corresponding vertex-degree Ramsey graph depends only on the partition of X into degree classes and may therefore admit additional automorphisms obtained by permuting vertices within the same class. Hence, in general, $\Phi(H_X) \subseteq Aut(G_X)$.

The symmetry considerations developed above impose strong structural constraints on the vertex-degree Ramsey graph G_X, which are directly responsible for the Ramsey-type result established in Section 2.1. Since the coloring is entirely determined by vertex degree, the set X is partitioned into degree classes, and the resulting graph is a complete bicolored graph in which edges within each class are green, while edges between distinct classes are red. This induces a semi-transitive structure: the green relation is an equivalency relation, whereas the red relation encodes its complement. Such a restricted class of colorings is far from arbitrary. In particular, when $|X| \geq 5$, these structural constraints force the appearance of a monochromatic triangle. Therefore, the Ramsey property in vertex-degree graphs should be understood as a geometric–combinatorial consequence: the tessellation, through its symmetry and degree distribution, generates a constrained coloring in which Ramsey-type substructures are unavoidable. Now consider one more example.

Example 2. Regular square tessellation

Consider the regular square tessellation (wallpaper group *p4m*). All vertices have degree 4. Hence $V(T) = C_4$ for any choice $X \subset V(T)$, consequently all edges are green. Thus, $G_X = K_n$ is the complete green clique, and $Aut(G_X) = S_n >> \Phi(H_X)$. Now consider two possibilities of the vertices choice:

Case A: symmetric choice. Let X be vertices of a square, in this case $H_X \cong D_4$. $\Phi(H_X) \subseteq Aut(G_X)$.

Case B: generic choice. We pick 5 random vertices. In this case $H_X = \{e\}$, but $Aut\{G_X\} \neq \{e\}$. This demonstrates that the symmetry of the graph does not come from geometry, but from degree degeneracy.

We conclude that the automorphism group of the vertex-degree graph is determined not by geometric symmetry, but by the multiplicities of degree classes; thus, it reflects degeneracy rather than geometry.

2.4. Vertex Type Ramsey Graphs Generated by Tessellations

Now we address vertex type generated by tessellations. We distinguish between two levels of geometric detail.

Definition 3. Vertex type invariants: multisets and sequences

For every vertex from set $X = \{v_1, \dots, v_n\} \subset V(T)$, we define its vertex type using one of the following invariants: vertex multiset $M(v_i) = \{\ell_1, \dots, \ell_m\}$ – an unordered collection of the number of sides ℓ of the m polygons meeting at v_i (Figure 2). This represents a relaxed invariant that ignores the spatial arrangement of the cells. And vertex symbol $\sigma(v_i) = (\ell_1, \dots, \ell_m)$, defined as the ordered sequence of polygons meeting at vertex v_i. This invariant preserves the spatial orientation of the cells.

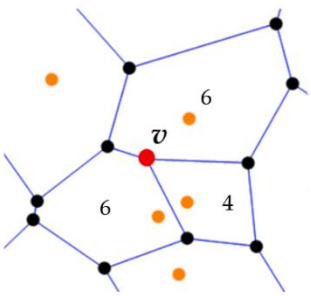

Figure 2. Vertex v of the type corresponding to the multiset $\{6, 6, 4\}$ is depicted as a red point. Orange points are the seeds of Voronoi tessellation.

Definition 4. Definition of the vertex type graph

 doi:10.20944/preprints202606.0392.v1

Choose a finite set of vertices $X = \{v_1, \dots, v_n\} \subset V(T)$ from the given tessellation T. We construct the complete graph G on these vertices, and color each edge $\{v_i, v_j\}$ as follows:

$$col_{ij}(v_i, v_j) = \begin{Bmatrix} \text{green, if two vertices have the same vertex type,} \\ \text{red, otherwise} \end{Bmatrix}, \quad (10)$$

where col_{ij} is the coloring function, and the "same vertex type" is determined by the equality of chosen invariants: $\mathrm{M}(v_i) = M(v_j)$ or $\sigma(v_i) = \sigma(v_j)$. Thus, the tessellation generates a complete bicolored graph $G_X = \{X, E, col\}$, where $E = \{\{v_i, v_j\}: i \neq j\}$, and *col* is the above coloring rule. Thus, a complete, bicolored, vertex-type Ramsey graph (VTG) emerges. The Ramsey-type theorem immediately emerges.

Theorem 3. Ramsey theorem for vertex-type graphs generated by tessellations.

Let T be a plane tessellation, and let $X = \{v_1, \dots, v_n\} \subset V(T)$ be a finite set of vertices. To every vertex v_i assign its vertex invariant (either the multiset $\mathrm{M}(v_i)$ or the vertex symbol $\sigma(v_i)$). Construct the complete graph $G = G(X, E, c)$, where $E = \{\{v_i, v_j\}: i \neq j\}$, and color every edge by:

$$col_{ij}(v_i, v_j) = \begin{Bmatrix} \text{green, if } \mathrm{M}(v_i) = M(v_j) \text{ or } \sigma(v_i) = \sigma(v_j), \\ \text{red, otherwise} \end{Bmatrix}.$$

Then every vertex-type graph G_X with $|X| \geq 5$ contains a monochromatic triangle. Moreover, the bound is sharp: there exist vertex-type graphs on four vertices with no monochromatic triangle.

Proof

The relation $v_i \sim v_j \leftrightarrow \mathrm{M}(v_i) = M(v_j) \vee \sigma(v_i) = \sigma(v_j)$, is an equivalence relation. Hence, the green edges form disjoint complete subgraphs corresponding to the equivalence classes of equal vertex types. Red edges connect vertices belonging to different equivalence classes. Now take five vertices. If at least three vertices have the same vertex type, they form an green triangle. If no three vertices share a common vertex type, then the five vertices are distributed among classes of size at most two. Therefore, at least three vertices must belong to three distinct vertex-type classes. The edges between them are all red, and hence they form a red triangle. Thus every G_X with five vertices contains a monochromatic triangle.

Thus, vertex-type Ramsey graphs generated by tessellations obey the same sharp 5-vertex monochromatic-triangle theorem as vertex-degree Ramsey graphs. The reason is that both constructions are induced by equality of a local combinatorial invariant: vertex degree in the former case, and vertex type in the present case.

3. Practical Implementation and Numerical Results

3.1. Computational Framework and Coloring Rules

The proposed concepts are illustrated through the analysis of random Voronoi tessellations. The numerical generation of Voronoi tessellations and the subsequent construction of the associated Ramsey graphs were implemented using Python. The statistical analysis of the generated data, including curve fitting and visualization of results, was performed using Wolfram Mathematica.

Let $S = \{s_i\}_{i \in I} \subset \mathbb{R}^n$ be a discrete set of distinct points, called generators, sites, or seeds. For every generator $s_i \in S$, we define its Voronoi cell by: $V_i = x \in \mathbb{R}^n: \|x - s_i\| \leq \|x - s_j\|, \forall j \neq I$, where $\|\cdot\|$ denotes the Euclidean norm. The collection $\mathcal{V}(S) = \{V_i\}_{i \in I}$ is called the Voronoi tessellation (or Voronoi diagram) generated by the set S. We consider a set of N random generator points distributed uniformly within a square domain $[0, L]^2$ under periodic boundary conditions, topologically equivalent to a torus. Periodic boundary conditions are necessary to avoid boundary effects on graph edges and polygon sets.

The Voronoi diagram partitions the torus into N distinct cells. The cell corresponding to a generator s comprises all points in the space that are closer to s than to any other generator. The vertices of these cells—defined as the points equidistant from three or more generators — constitute the set of nodes V of the spatial tessellation T. For a standard Voronoi tessellation on a plane, the number of nodes is given by $n = |V| = 2N$.

 doi:10.20944/preprints202606.0392.v1

We construct a complete graph G_n on the vertex set V. For every edge $\{v_i, v_j\} \in E(G_n)$, we apply a coloring function based on four rules: one VDG and three VTG rules (MEG, SEG, and SIG). For each classification rule, we analyze the following structural and statistical characteristics:

- The percentage of green edges p.
- The distribution and total number *K* of equivalence classes.
- The maximum clique size ω within the green and red subgraphs.
- The transitivity violation count *TV* (instances where $\{v_i, v_j\}$ and $\{v_i, v_k\}$ are green, but $\{v_k, v_w\}$ is red).
- Turán number estimations and the analysis of rule-specific trends.

Then we will analyze asymptotic estimations. The applied rules are following:

1) *Rule 1. VDG (Vertex-Degree Graph)*

Since we assume a standard non-degenerate Voronoi diagram where exactly three cells meet at each vertex, all nodes have a degree of three. Consequently, under the VDG rule, the entire complete graph G_n becomes green $p_{\mathrm{VDG}} = 100\%$, number of equivalence classes $K_{\mathrm{VDG}} = 1$, $TV_{\mathrm{VDG}} = 0$. The maximum green and red clique sizes are $\omega_{\mathrm{gr},1} = n$, $\omega_{\mathrm{red},1} = 0$. Although this rule is degenerate, it serves to validate the computational implementation.

2) *Rule 2. MEG. Graph Based on Multiset Identity (Multiset-Equivalence Graph (MEG))*

An edge $\{v_i, v_j\} \in E(G_n)$ is colored according to color function Eq. 10, the node type is defined by its multiset of adjacent cell types $M(v_i)$. This rule defines a rigorous equivalence relation. The green edges partition the vertex set V into disjoint equivalence classes (cliques), ensuring that no transitivity violations occur. That means that $TV_2 = 0$.

3) *Rule 3. SEG. Graph Based on Ordered Sequences (Sequence-Equivalence Graph (SEG))*

This rule refines Rule 2 MEG by incorporating spatial orientation and clockwise (or counter-clockwise) traversal order of the adjacent cells surrounding the node. In other words, we use vertex symbol $\sigma(v_i)$ in Eq. 10. This rule imposes a stricter geometric symmetry requirement than the unordered multiset identity.

4) *Rule 4 SIG. Graph Based on Non-Empty Set Intersection (Set Intersection Graph (SIG))*

An edge $\{v_i, v_j\} \in E(G_n)$ is colored *green* if the multisets of the two nodes possess a non-empty intersection: $M(v_i) \cap M(v_j) \neq \emptyset$. This rule relaxes the strict identity requirement of Rule 2 MEG. Since a single cell type can link distinct multisets, this relation is non-transitive, resulting in transitivity violations and the formation of complex, overlapping cluster structures rather than disjoint cliques.

In the following formulas we will use the number of the rules as its index.

3.2. Statistical Distribution of Cell Types and Vertex Neighborhoods

First, the distribution of cell types ℓ and the node neighborhoods $M(v)$ must be determined (see Appendix A, Figures 1A, 2A). While no analytical solution exists for the Voronoi distribution, numerous studies have provided similar calculations for cell distribution [14].

3.3. Analysis of Rule 2 MEG

The exact formulas for the number of green and red edges can be derived using 2-combinations of class sizes:

$$E_{\mathrm{green},2} = \sum_{i=1}^{K_2} \binom{m_i}{2} = \frac{1}{2}\left(\sum_i m_i^2 - \sum_i m_i\right) = \frac{1}{2}\left(\sum_i m_i^2 - n\right), \tag{11}$$

$$E_{\mathrm{red},2} = \binom{n}{2} - E_{\mathrm{green},2} = \sum_{i<j} m_i\, m_j = \frac{n^2 - \sum_i m_i^2}{2},$$

where m_i – the size of the class $\widetilde{M}_i$, K_2 is the number of all the classes $\widetilde{M}$. We used the simple fact that the sum of the class sizes is equal to number of nodes: $\sum_i m_i = n$.

 doi:10.20944/preprints202606.0392.v1

To analyze the statistical behavior, we rewrite Eq. 11 in terms of the mean class size μ and the biased variance σ^2:

$$\mu = \frac{1}{K_2}\sum_i m_i = \frac{n}{K_2}, \tag{12}$$

$$\sigma^2 = \frac{1}{K_2}\sum_i m_i^2 - \mu^2 \quad \Rightarrow \quad \sum_i m_i^2 = K_2(\sigma^2 + \mu^2). \tag{13}$$

Equations 11 through Eq. 12,13 become:

$$E_{\text{green},2} = \frac{1}{2}(K_2(\sigma^2 + \mu^2) - n) = \frac{n}{2}\left(\frac{\sigma^2}{\mu} + \mu - 1\right),$$

$$E_{\text{red},2} = \frac{n}{2}(n - \mu - \frac{\sigma^2}{\mu}). \tag{14}$$

This indicates that a greater dispersion (variance) in equivalence class sizes (see Figure 5B) directly increases the number of green connections.

Accordingly, the fraction of green connections:

$$p_2 = \frac{n}{2}(\frac{\sigma^2}{\mu} + \mu - 1)/(\frac{n(n-1)}{2}) = \frac{1}{n-1}(\frac{\sigma^2}{\mu} + \mu - 1). \tag{15}$$

To characterize the asymptotic behavior, p_2 is estimated using simple combinatorial arguments: if we have K_2, in which we have in average $\binom{\mu}{2}$ connections, then:

$$p_2 = \frac{E_{\text{green},2}}{\binom{n}{2}} \approx \frac{K_2\binom{n/K_2}{2}}{\frac{n(n-1)}{2}} \approx \frac{K_2\frac{(n/K_2)^2}{2}}{\frac{n^2}{2}} = \frac{1}{K_2}. \tag{16}$$

Empirically, K_2 is observed to grow logarithmically with n (Figure 3B). This fact enables the following estimation. where the number of classes is interpreted similarly to number of Boltzmann states (see Figure 9 for p in log-log scale).

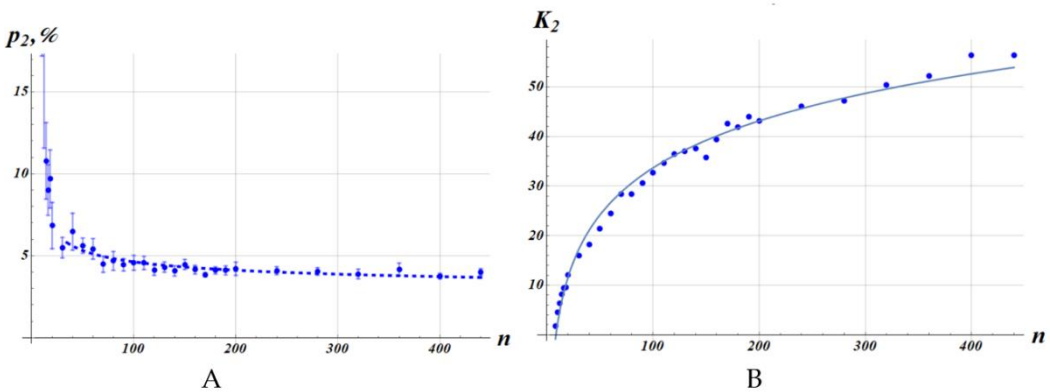

Figure 3. A) The fraction of green links in MEG graph with fitting $p_2 \approx 17.97/\ln(n) + 0.73$, $R^2 = 0.996$. B) Number of classes K_2 with logarithmic fitting $K_2 \approx 13.66\ln(n) - 29.23$, $R^2 = 0.998$.

Now we consider the clique formation. The green graph is a set of cliques. The red graph is a complete graph. The maximum green clique size corresponds to the maximum class size: $\omega_{\text{green},2} = \max(m_i)$. Maximal red clique is equal to number of classes (we choose one node from each class): $\omega_{\text{red},2} = K_2$.

How can $\omega_{\text{green},2}$, be estimated from the average class size μ? Considering it as a deviation from the mean, $\mu + \beta\sigma$, and compare the real β with its normal distribution estimation (see Figure 4), allows for a better understanding of the graph's topological structure.

 doi:10.20944/preprints202606.0392.v1

For normal distribution for large number of independent (it's not like that) clique sizes maximum asymptotic gives $\beta_{\text{theory}} = \sqrt{2\ln K_2}$. For $n > 50$ relation between β is $\beta_{\text{real}}/\beta_{\text{theory}} > 1$ (Figure 5A). This clearly demonstrates that the system exhibits structural order, with nodes being unevenly distributed among classes. The significant deviation from the mean μ compared to a random graph suggests that a dominant class (ideally {6, 6, 6}) imposes its structure on the remaining nodes. If the relation between β were less than one, then one could say that the variance of the classes would be small. The class sizes would be almost the same. The presence of one domain prevents adjacent domains from sharing the same type.

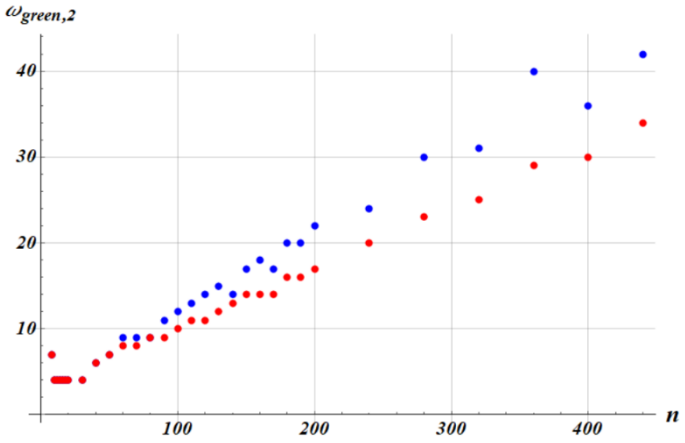

Figure 4. The maximum size of clique in the green MEG subgraph. Blue points – the real ones, the red – estimation $\omega_{\text{green},2} \approx \mu + \beta_{\text{theory}}\sigma$.

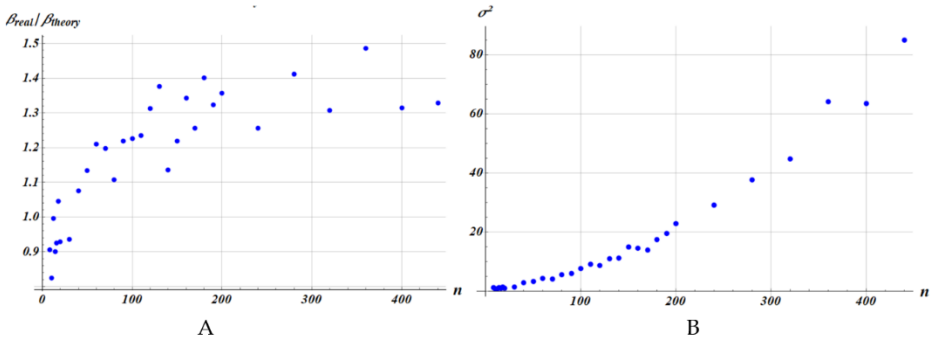

A B

Figure 5. A) The relation between coefficient β_{real}, calculated directly from data, and estimated one β_{theory}. B) The variance of the sizes of equivalence classes.

Using the approximation for K_2, we can estimate Ramsey-type threshold: the number of nodes n at which a red clique of size K_2 is expected to appear. It is $n \approx e^{\frac{K_2 - b}{a}}$:

Table 1. Ramsey threshold estimation.

K_2 (red clique size)	Estimated n
3	15
4	16
5	17
6	17
10	21

Finally, we provide estimation for Turán number and compare it with direct calculations. The exact formula for Turán number – the maximal number of edges in subgraph $K_{\omega+1}$ on n nodes:

Preprints.org (www.preprints.org) | NOT PEER-REVIEWED | Posted: 4 June 2026 doi:10.20944/preprints202606.0392.v1

$$T(n,w) = \sum_{0\le i<j\le w-1} \left[\frac{n+i}{w}\right]\left[\frac{n+j}{w}\right]. \quad (17)$$

We will consider the relation:

$$Tr_{\text{green},2} = \frac{E_{\text{green},2}}{T(n,\omega_{\text{green},2})}. \quad (18)$$

Considering Eq 16: $E_{\text{green},2} = p_2\binom{n}{2} \approx p_2\frac{n^2}{2}$, and upper bound for Turán number: $(1 - 1/\omega)\cdot n^2/2$ we get:

$$Tr_{\text{green},2} = \frac{E_{\text{green},2}}{T(n,\omega_{\text{green},2})} \approx \frac{p_2\omega_{\text{green},2}}{\omega_{\text{green},2}-1} \xrightarrow{n\to\infty} 0 \quad (19)$$

tending to zero (logarithmically slow) as K_2 becomes big (Figure 6A).

For the red graph:

$$Tr_{\text{red},2} = \frac{E_{\text{red},2}}{T(n,\omega_{\text{red},2})} \xrightarrow{n\to\infty} 1, \quad (20)$$

that is, the classes in this approximation are divided into commensurate groups, and the graph approaches the Turán graph (empirically 0.976).

Through mean and variance:

$$Tr_{\text{green},2} = \frac{\frac{\sigma^2}{\mu}+\mu-1}{n-1}\frac{\mu+\beta\sigma}{\mu+\beta\sigma-1}, \quad (21)$$

$$Tr_{\text{red},2} = \frac{E_{\text{green},2}}{T(n,\omega_{\text{green},2})} = \left(\frac{n}{2}\left(n-\mu-\frac{\sigma^2}{\mu}\right)\right)\Big/\left(\left(1-\frac{\mu}{n}\right)\frac{n^2}{2}\right) = 1-\frac{\sigma^2}{\mu(n-\mu)}.$$

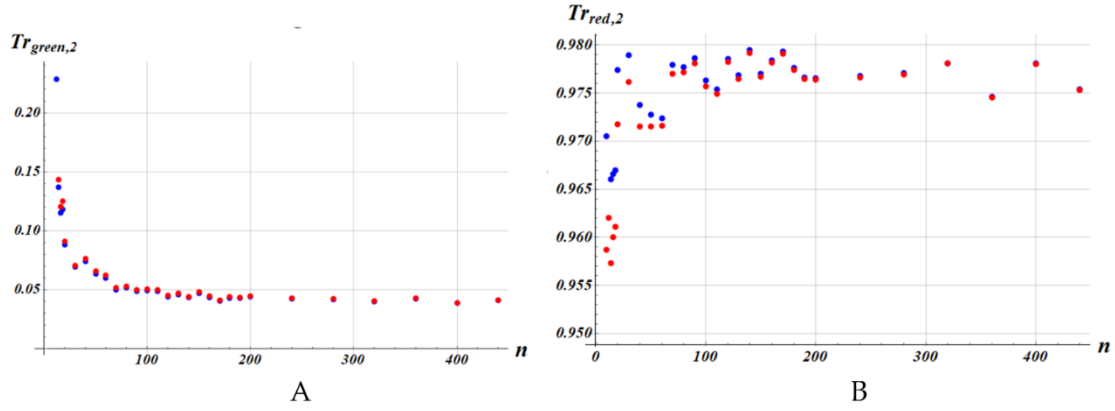

Figure 6. A) Turán ratio for MEG green subgraph. B) Turán ratio for MEG red subgraph. Blue points correspond to directly calculated Turán number (Eq. 17), red ones – to estimation (Eq. 19, 20).

3.4. Analysis of Rule 3 SEG

We now consider the ordering within MEG classes. Triples that cannot be mapped onto each other via cyclic shifts (e.g. (5, 6, 7) and (5, 7, 6)) are partitioned into two distinct classes. The only classes in MEG that split up are the ones in which all three types of cells ℓ are different. We will consider such a vertex symbol as chirality property (Figure 7).

This rule is identical to the MEG, so the previous estimations are the same, only number of classes is different. Since $K_3 > K_2$, the following relations hold: $p_3 < p_2$, $\omega_{\text{green},3} < \omega_{\text{green},2}$, $\omega_{\text{red},3} > \omega_{\text{red},2}$, $Tr_{\text{green},3} < Tr_{\text{green},2}$,. $Tr_{\text{red},3} < Tr_{\text{red},2}$ (see Appendix B).

Empirical results indicate that approximately half of MEG classes are chiral: $K_3 \approx K_2 + \frac{K_2}{2}$. Then $\frac{K_3-K_2}{K_3} \approx 1/3$, what is seen from the strict calculation (Figure 8). This is due to the distribution of polygons q_ℓ. The probability of a chiral node (estimated for independent cells) is given by:

 doi:10.20944/preprints202606.0392.v1

$$PrChir = 1 - Pr(a,a,a) - Pr(a,a,b), \tag{22}$$

$$Pr(a,a,a) = \sum_k q_k^3 = 0.053$$

$$Pr(a,a,b) = 3\sum_{k\neq l} q_l q_k^2 = 0.48$$

$$PrChir \equiv Pr(a,b,c) = 6\sum_{k\neq l\neq m} q_k q_l q_m = 0.46$$

The empirical value is slightly higher (~+4%), as there is a correlation of neighboring cells.

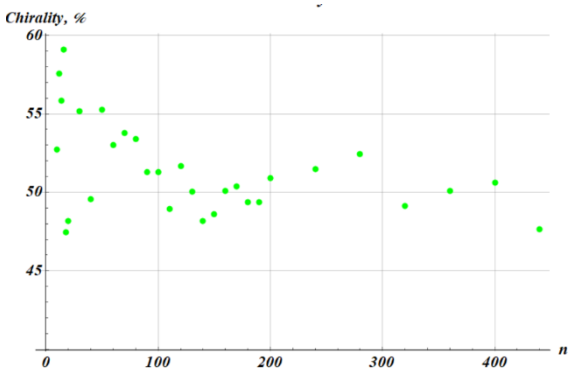

Figure 7. Percentage of the chiral nodes.

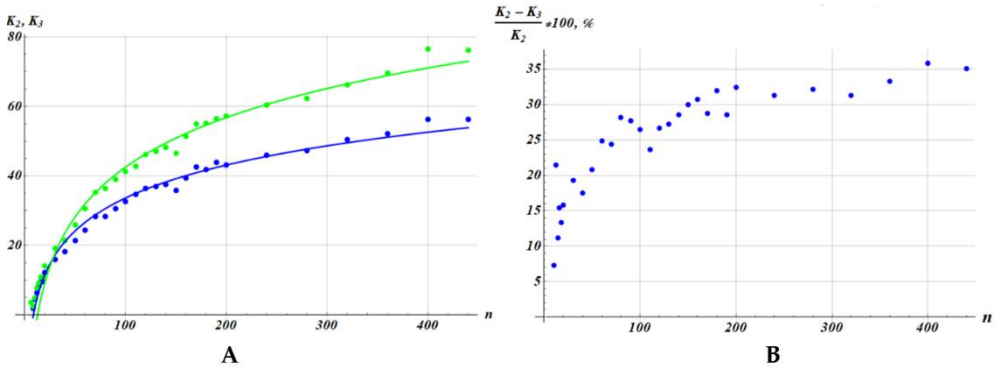

Figure 8. A) Number of classes K_2 with logarithmic fitting $K_2 \approx 13.66\ln(n) - 29.23$, $R^2 = 0.998$; $K_3 \approx 20.59\ln(n) - 52.24$, $R^2 = 0.998$. B) Relative relation between K_2 and K_3.

3.5. Analysis of Rule 4 SIG

For large n, the fraction of green connections p_4 approaches to a constant value. It means that $M(v_i) \cap M(v_j)$ depends on distribution q_ℓ only, and independent on n. We denote this asymptotic value as p_4^*.Empirically it's 85.7±0.4% (see Figure 9).

Now we will estimate p_4^* in three ways. A lower bound can be established by assuming that primary connections arise from the presence of at least one hexagon in $M(v_i)$:

$$p_4^* \geq (Pr(6))^2 = (1 - (1 - q_6)^3)^2 \approx 42\%, \tag{23}$$

where $Pr(6)$ – is probability that in $M(v_i)$ at least one hexagon.

Let's denote the number of common ℓ for two nodes: $|M(v_i) \cap M(v_j)| = N_{ij}$. Then the expectation is:

$$\mathrm{E}(N_{uv}) = \sum_\ell Pr(\ell \epsilon M(v_i)) Pr(\ell \epsilon M(v_j)) = \sum_\ell Pr(\ell \epsilon M)^2 = \lambda.$$

 doi:10.20944/preprints202606.0392.v1

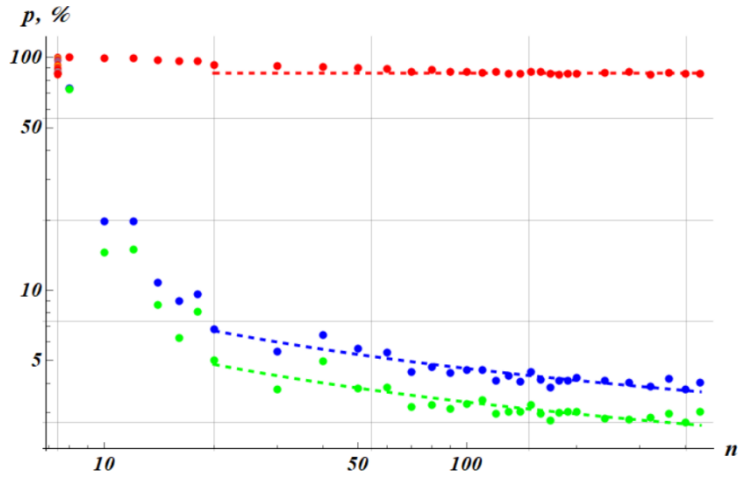

Figure 9. The fraction of green links p in log-log scale for three rules: blue – rule 2 MEG, green – rule 3 SEG, red – rule 4 SIG. Dashed lines correspond to logarithmic fitting for rules 2 and 3, and constant for rule 4: $p_2 \approx 17.97/\ln(n) + 0.73$, $R^2 = 0.996$; $p_3 \approx 12.85/\ln(n) + 0.53$, $R^2 = 0.993$; p_4^* =85.7±0.4%.

If we assume that q_ℓ has Poisson distribution, then expectation $\lambda = \sum_\ell (1-(1-q_\ell)^3)^2 \approx 1.16$. The next estimation for p_4^*:

$$p_4^* = 1 - Pr(N_{ij} = 0) = 1 - \frac{\lambda^0}{0!} e^{-\lambda} \approx 68.7\% \quad (24)$$

It is well-established that Voronoi tessellations do not follow a Poisson distribution, as there is a correlation between cell types (5-gon and 7-gon come with hexagon more often). So, it is not a random distribution. It's closer to sub-Poisson distribution as variance of N_{ij} is less than expectation λ:

$$\sum_\ell Pr^2(\ell \epsilon M)(1 - Pr^2(\ell \epsilon M)) = 0.79 < \sum_\ell Pr(\ell \epsilon M)^2 = \lambda = 1.16.$$

That is, the intersections of the types are distributed closer to the average than in the random case. Deviation from Poisson distribution $1 - 0.79/1.16 \approx 0.32$ corresponds to correlation between cells.

More precise approach is considering independent cell type combinations, forming M. It is easier to calculate that two nodes don't have intersection ($N_{ij} = 0$):

$$p_4^* = 1 - \sum_{A,B;A\cap B=\emptyset} P(M = A)P(M = B), \quad (25)$$

$$P(M = A) = \sum_{M\sim A} \frac{3!}{\prod_{\ell \in A} m_\ell!} \prod_{k \in A} q_k^{m_\ell},$$

where $P(M = A)$ is just a sum of permutations of elements in the multiset, taking into account multiplicity m, multiplied by the probability of a specific combination of types falling out over all multisets of M with types from A. Calculation shows $p_4^* = 0.8432$ (84.3%).

This estimate is in close agreement with a Monte Carlo simulation performed for 10^5 pairs. Simulated $p_4^* = 0.844$ (84.4%). The difference between empirical value (~1.3%) is caused by correlation presence. The estimated values of p_4^* are depicted in Figure 10.

 doi:10.20944/preprints202606.0392.v1

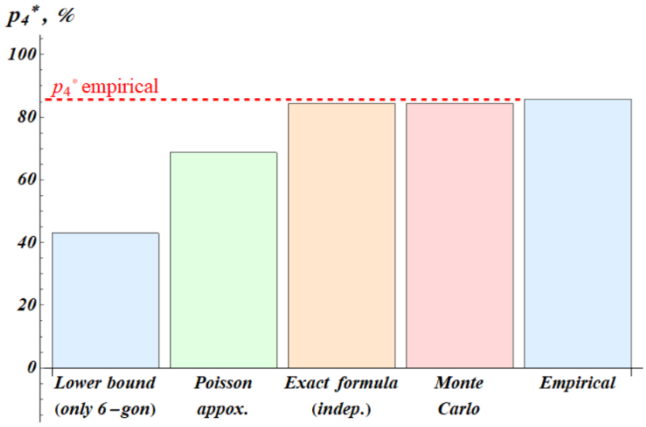

Figure 10. Four p_4^* estimations: lower bound (Eq. 23), Poisson approximation (Eq. 24), q_ℓ multiset combinations (Eq. 25), Monte Carlo. Blue bar is the empirical value.

Finally, knowing p_4^* we can estimate transitivity violation TV_4. The number of violating ordered links triples (*i, j, k*), that is, such that *ij* is green, *jk* is green, *ik* is red (random graph approximation):

$$TV_4 = n(n-1)(n-2)p_4^{*2}(1-p_4^*)/6 \sim C \cdot n^3. \quad (26)$$

It describes the empirical data quite well (Figure 11): the fitted constant $C = 3.7 \cdot 10^{-2}$, $R^2 = 0.9996$, as $p_4^{*2}(1-p_4^*)/6 = 3.25 \cdot 10^{-2}$. Relative difference is 0.14.

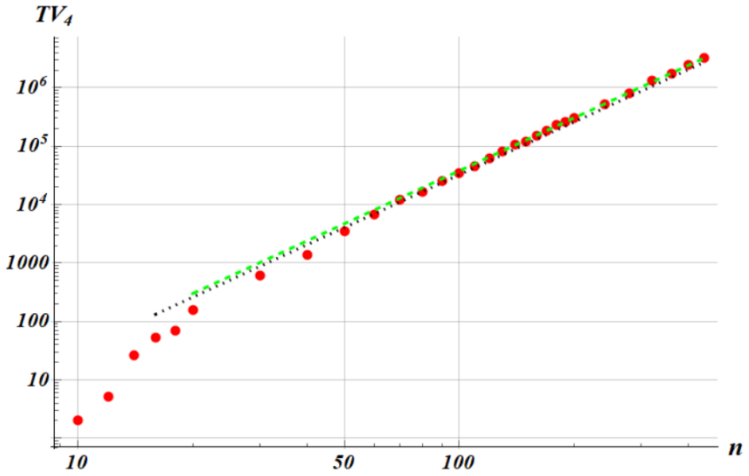

Figure 11. Red point: strict computational counting. Green dashed line: fitting with Eq. 26 ($C = 3.7 \cdot 10^{-2}$, $R^2 = 0.9996$). Black dotted line: Eq 26 with constant $p_4^{*2}(1-p_4^*)/6 = 3.25 \cdot 10^{-2}$.

Green and red cliques

Calculating the maximum green clique is an NP-hard problem. In the program we tried to estimate the lower bound going along the nodes with maximal connections number. We will see that we can consider it quite close to the real value, since we actually going through all the nodes containing hexagon – the maximum clique.

Theoretically we should take q_M and find all M containing the most frequent polygon (hexagon) and sum up the probabilities:

$$\omega_{green,4} = n * \sum_{M \ni \ell=6} q_M. \quad (27)$$

This perfectly matches the program calculation (Figure 12). We see a linear relationship. The slope (sum of probabilities) is 0.66 (66% of all nodes contain at least one hexagon).

Preprints.org (www.preprints.org) | NOT PEER-REVIEWED | Posted: 4 June 2026 doi:10.20944/preprints202606.0392.v1

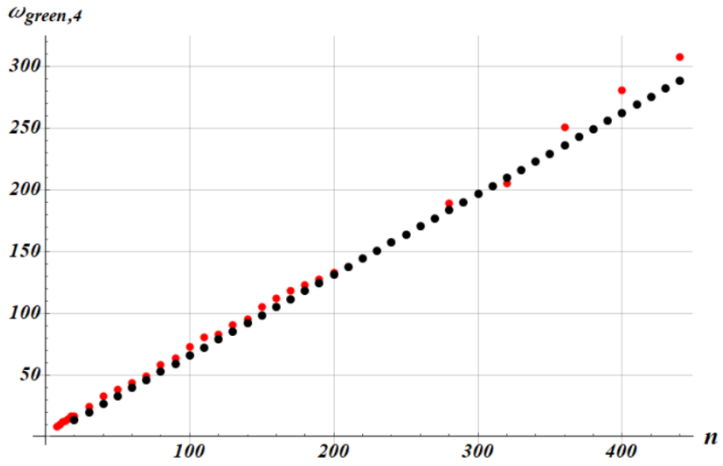

Figure 12. Red points: results of a "greedy algorithm". Black points: estimation with Eq. 27.

The red clique for large n is constant and equals 3:

$$\omega_{\mathrm{red},4} = 3. \tag{28}$$

This can be understood in terms of the Pigeonhole Principle (or Dirichlet's box principle). If we consider a multiset {3, 4,..., 12} with equally probable elements, then we place triples with identical elements in Dirichlet boxes. Then the maximum click is 10 (number of types: 12-3+1). In reality, this does not happen because of the q_ℓ distribution. We have to think about Dirichlet boxes, which consume three different elements that do not repeat in other boxes. Maximum: 10/3~3 (Figure 13).

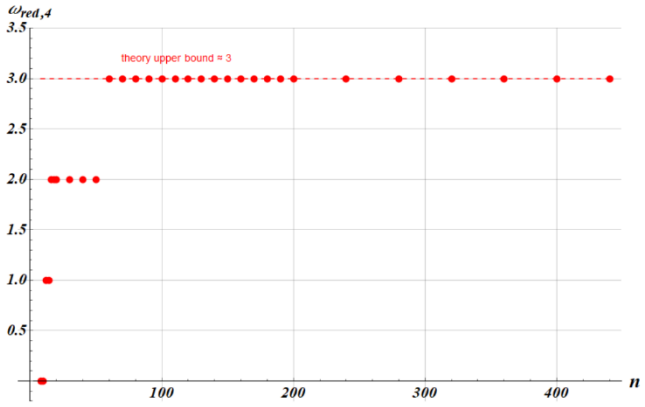

Figure 13. Maximal red clique values.

Turán ratio

From Eq. 27 we can approximate $T(n, w_{\mathrm{green},4}{\sim}n) \approx n^2/2$, therefore:

$$\mathrm{Tr}_{\mathrm{green},4} = \frac{E_{\mathrm{green},4}}{T(n, w_{\mathrm{green},4})} \approx \frac{p_4^* n^2/2}{n^2/2} = p_4^*, \tag{29}$$

what matches empirical data (Figure 14).

 doi:10.20944/preprints202606.0392.v1

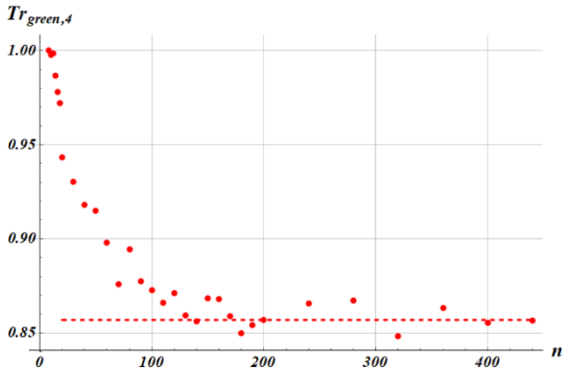

Figure 14. Red points: empirical Turán ratio data. Red dashed line: the asymptotics according to Eq. 29.

For Turán ratio in red subgraph, we only have to estimate number of red connections: $E_{\mathrm{red},4} \approx (1-p_4^*)n(n-1)/2$. Turán number: $T(n,3) \approx n^2/3$. Consequently:

$$\mathrm{Tr}_{\mathrm{red},4} \approx \frac{3(1-p_4^*)}{2} = \frac{3}{2}p_{\mathrm{red}}, \tag{30}$$

where p_{red} is a fraction of red connections.

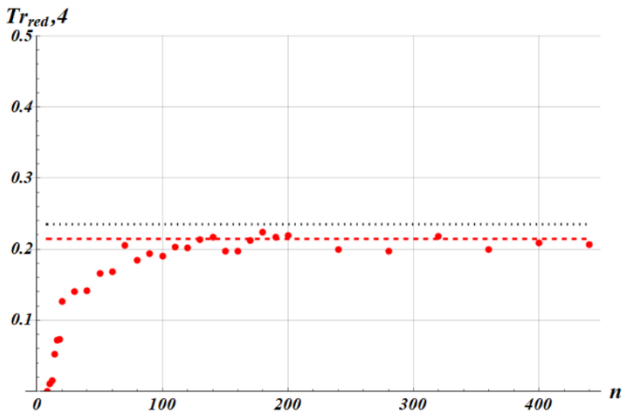

Figure 15. Red points: empirical values. Red dashed line: asymptotic corresponding to Eq. 30 with empirical p_4^*. Black dashed line: Eq. 30 with analytical p_4^*.

Discussion

The present work introduces a new class of structured Ramsey graphs generated intrinsically by plane tessellations. In contrast to classical Ramsey theory, where edge colorings are arbitrary [6,7], the colorings studied here arise naturally from local geometric invariants, namely vertex degree and vertex type. This distinction is fundamental. The resulting graphs are not generic bicolored complete graphs but highly constrained, partition-generated structures in which one color corresponds to an equivalence relation. Consequently, the Ramsey properties established in the present work originate not from the randomness of the coloring but from the internal combinatorial organization imposed by tessellation geometry [31]. The introduced vertex-degree graphs (VDGs) and vertex-type graphs (VTGs) demonstrate that tessellations provide a natural geometric realization of equivalence-relation Ramsey structures. The obtained monochromatic-triangle theorem for five vertices has a particularly transparent combinatorial interpretation: among five values, either three coincide or three are pairwise distinct. Thus, the geometric Ramsey phenomenon reduces to a structural property of partitions. The tessellation serves as the geometric carrier of this combinatorial inevitability. An important feature of the introduced framework is the asymmetry between the two colors. In classical extremal graph theory, Turán-type optimization is usually formulated for a single graph class [7–9]. In the present setting, however, the two colors possess fundamentally different structural meanings. One color corresponds to equivalence classes and therefore generates disjoint cliques, whereas the

 doi:10.20944/preprints202606.0392.v1

complementary color connects distinct classes. As a result, the extremal configurations maximizing the two edge types cannot generally be realized simultaneously. This asymmetry constitutes a characteristic property of partition-generated Ramsey graphs and distinguishes them sharply from arbitrary two-colorings. The relation between geometric symmetry and graph symmetry also deserves attention. The symmetry group of the tessellation acts naturally on the associated Ramsey graph through preserving local invariants, such as valency and vertex type. However, the passage from tessellation to graph is not straightforward. The graph retains only partial geometric information, namely the partition into equivalence classes. Consequently, additional purely combinatorial automorphisms may emerge which are absent in the original tessellation. The obtained inclusion $\Phi(H_X) \subseteq \mathrm{Aut}(G_X)$ expresses this projection from geometric symmetry to combinatorial symmetry. The Cairo tiling illustrates this phenomenon particularly clearly: although the geometric stabilizer of a finite vertex subset may be trivial, the associated VDG may still possess nontrivial automorphisms generated by permutations within degree classes.

The practical implementation based on Voronoi tessellations further demonstrates that the introduced framework extends naturally beyond ideal periodic tilings [32]. Random tessellations generate rich statistical families of structured Ramsey graphs whose properties depend on distributions of local cell configurations. The distinction between equivalence-based rules (MEG, SEG) and non-transitive intersection-based rules (SIG) reveals the transition from partition-generated structures to genuinely non-transitive graph topologies with overlapping clusters and transitivity violations (see Table 2).

Table 2. Summary of Tessellation-Generated Ramsey Graph Rules.

Feature	VDG (Rule 1)	MEG/SEG (Rules 2 and 3)	SIG (Rule 4)
Equivalence relation	True	True	True
Transitivity	Transitive (TV=0)	Transitive (TV=0)	Non-transitive ($TV \sim O(n^3)$)
Graph Topology	Disjoint complete green cliques	Disjoint complete green cliques	Overlapping cluster structures
Asymptotic Green Fraction (p)	$p_1 = 100\%$	Decays logarithmically $p \sim 1/K;\ p_3 < p_2$	Approaches constant $p_4^* = 85.7 \pm 0.4\%$
Max Green Clique	$\omega_{green,1} = n$	Max size of equivalence class; $\omega_{green,3} < \omega_{green,2}$	Linear growth $\omega_{green,4} \approx 0.66n$
Max Red Clique	$\omega_{red,1} = 0$	$\omega_{red} = K;\ \omega_{red,3} > \omega_{red,2}$	Constant $\omega_{red,4} = 3$
Turán ratio	1	$Tr_{\mathrm{green}} \xrightarrow{n\to\infty} 0$, $Tr_{\mathrm{red}} \to 1$, $Tr_{\mathrm{green},3} < Tr_{\mathrm{green},2}$, $Tr_{\mathrm{red},3} < Tr_{\mathrm{red},2}$	$\mathrm{Tr}_{\mathrm{green},4} \approx p_4^*$, $\mathrm{Tr}_{\mathrm{red},4} \approx \frac{3}{2}(1 - p_4^*)$

In this sense, Voronoi tessellations provide a natural laboratory for studying structured Ramsey phenomena in disordered systems [32]. The present work opens several directions for future research. First, higher-dimensional generalizations may be developed for spatial tessellations and Voronoi decompositions in $\mathbb{R}^3$ and higher dimensions. Second, the framework may be extended from bicolorings to multicolor Ramsey structures generated by several local invariants simultaneously. Third, probabilistic versions of tessellation-generated Ramsey graphs may be investigated for stochastic geometric processes. Finally, the introduced approach suggests a broader principle: local geometric invariants naturally induce structured combinatorial colorings whose Ramsey properties

 doi:10.20944/preprints202606.0392.v1

reflect the interplay between geometry, symmetry, equivalence relations, and extremal graph theory [33].

5. Conclusions

A new class of structured Ramsey graphs, generated by plane tessellations, has been introduced and analyzed. Unlike classical Ramsey graphs, where edge colorings are arbitrary, the colorings considered in the present work arise intrinsically from local geometric invariants, namely vertex degree and vertex type. This construction leads naturally to partition-generated or semi-transitive complete bicolored graphs in which one color corresponds to an equivalence relation and forms disjoint cliques, while the complementary color connects distinct equivalence classes.

Within this framework, sharp Ramsey-type results were established for vertex-degree (VDG) and vertex-type graphs (VTG), where VTG includes both multiset (MEG) and sequence-based (SEG) implementations. In particular, every such graph on five vertices necessarily contains a monochromatic triangle. The resulting theorem possesses a straightforward combinatorial core: given five values, either three coincide or three are pairwise distinct. Thus, the Ramsey property emerges as a direct consequence of the partition structure induced by local tessellation invariants.

Turán numbers for the introduced structured colorings were calculated. In contrast to classical extremal graph theory, the two colors exhibit a fundamental asymmetry because they represent inequivalent combinatorial structures: equivalence-class cliques versus inter-class connections. The corresponding extremal configurations therefore cannot generally be realized simultaneously.

The relation between geometric symmetry of tessellations and combinatorial symmetry of the associated Ramsey graphs was also clarified. Tessellation symmetries induce graph automorphisms through preservation of local invariants; however, additional combinatorial automorphisms may emerge due to degeneracies of degree or vertex-type classes. Thus, the passage from tessellations to Ramsey graphs acts as a projection from geometry to combinatorics.

The practical implementation based on Voronoi tessellations demonstrated that the proposed framework extends naturally to random and disordered tessellations. Equivalence-based and non-transitive coloring rules were shown to generate qualitatively different graph topologies, ranging from disjoint clique structures to overlapping non-transitive cluster systems.

The present work bridges between tessellation geometry, equivalence relations, Ramsey theory, and extremal graph theory. More broadly, it suggests that local geometric invariants constitute a natural source of structured Ramsey colorings, in which combinatorial inevitability arises from intrinsic geometric organization rather than arbitrary edge assignment.

Author Contributions: Conceptualization, E. B.; A.G. and S.S.; methodology, E. B.; A.G. and S.S.;.software**,** A.G.; validation, A.G.; E.B. and A. G.; investigation, E. B.; A.G. and S.S.

Funding: This research received no external funding.

Data Availability Statement: The original contributions presented in this study are included in the article. Further inquiries can be directed to the authors.

Conflicts of Interest: The authors declare no conflicts of interest.

Abbreviations

The following abbreviations are used in this manuscript:

MDPI	Multidisciplinary Digital Publishing Institute
DOAJ	Directory of open access journals
MEG	Multiset-Equivalence Graph
SEG	Sequence-Equivalence Graph
SIG	Set Intersection Graph
TV	Transitivity Violation

 doi:10.20944/preprints202606.0392.v1

VDG Vertex-Degree Ramsey Graph
VTG Vertex-Type Ramsey Graph

Appendix A

Appendix A.1

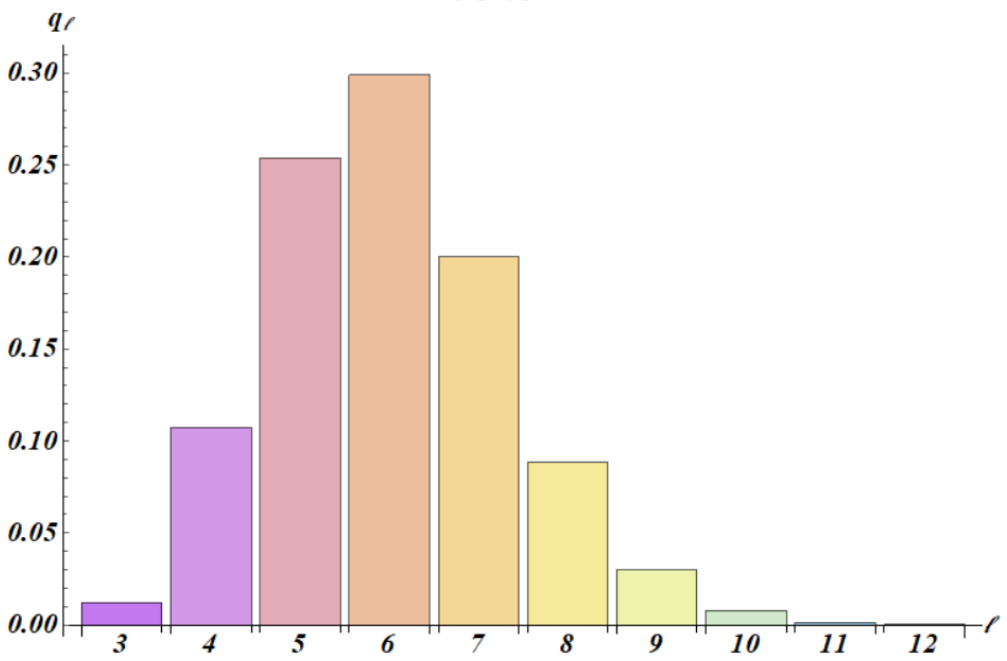

Figure A1. Distribution of cell types ℓ.

Table A1. Comparative table for computational distribution q_ℓ and q_ℓ reported by Calka [14].

ℓ	q_ℓ	q_ℓ by Calka [14]
6	0.29895	0.29473
4	0.107502	0.106838
8	0.0882781	0.0897
5	0.253834	0.25946
7	0.20026	0.19877
3	0.0121601	0.01124
9	0.0296985	0.0295
10	0.00767202	0.00743
11	0.00135112	0.00149
12	0.000293722	0.00025

Preprints.org (www.preprints.org) | NOT PEER-REVIEWED | Posted: 4 June 2026 doi:10.20944/preprints202606.0392.v1

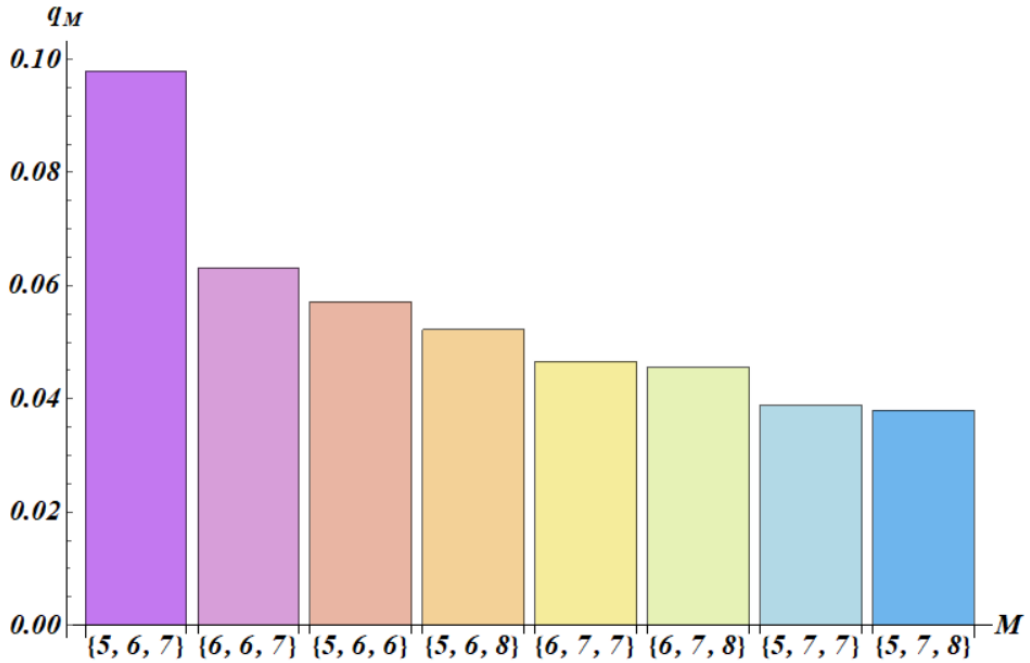

Figure A2. Distribution of multisets *M*.

Appendix B

Results for corresponding values $\omega_{\text{green},3} < \omega_{\text{green},2}$, $\omega_{\text{red},3} > \omega_{\text{red},2}$, $Tr_{\text{green},3} < Tr_{\text{green},2}$, $Tr_{\text{red},3} < Tr_{\text{red},2}$.

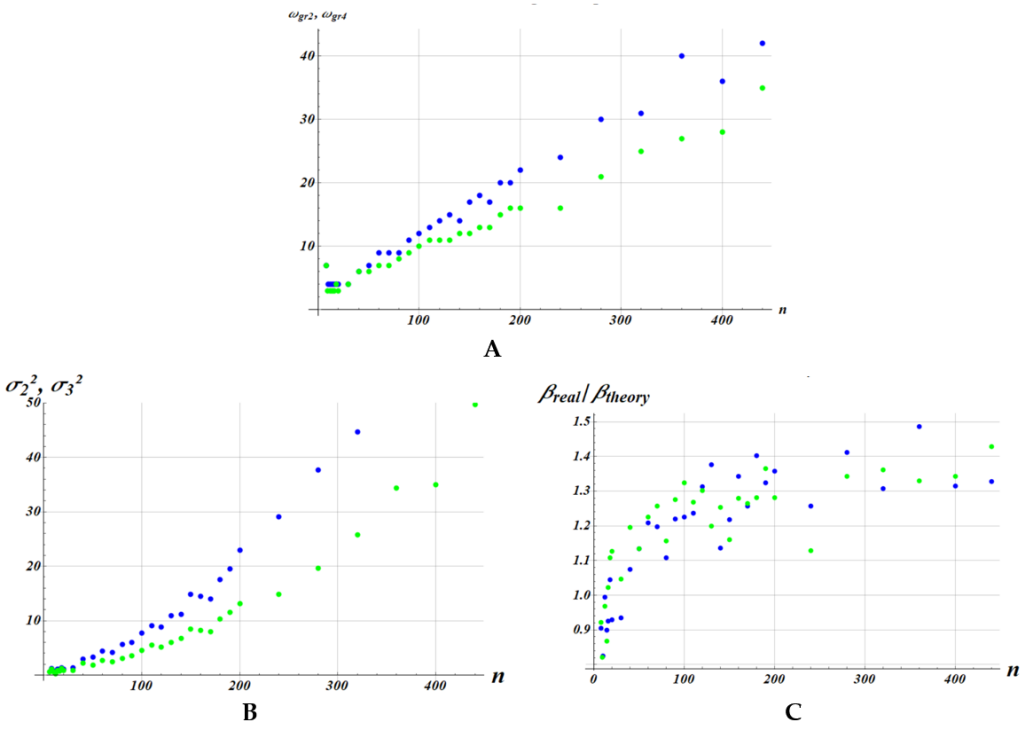

Figure 1. A) Maximal green clique size ω_{green}, B) variance of classes σ^2 and C) $\beta_{\text{real}}/\beta_{\text{theory}}$ for MEG (blue) and SEG (green) rules.

 doi:10.20944/preprints202606.0392.v1

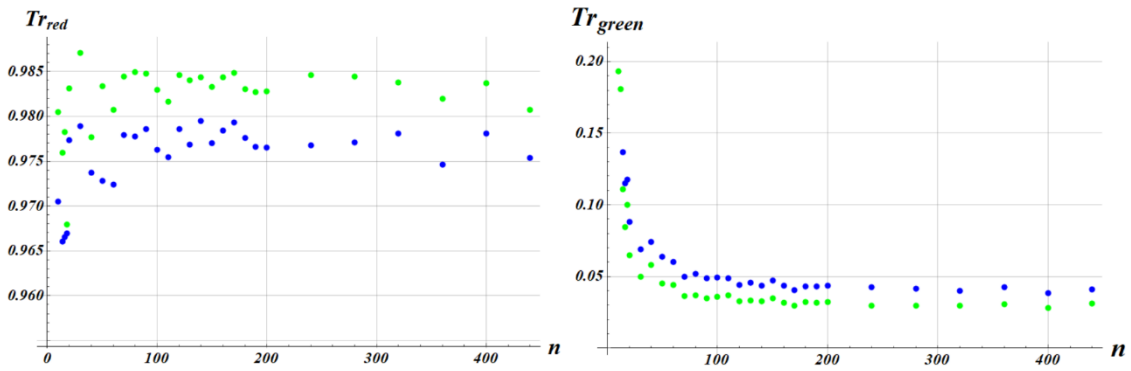

A B

Figure 2. Turán ratio for green (A) and red (B) subgraphs for MEG (blue) and SEG (green) graphs.

Table 1. Ramsey threshold estimation.

K_2 (red clique size)	K_3	Estimated n
3	11	15
4	12	16
5	13	17
6	14	17
10	18	21

References

1. Grünbaum, B.; Shephard, G.C. *Tilings and Patterns*; W.H. Freeman: New York, NY, USA, 1987;
2. Conway, J.H.; Burgiel, H.; Goodman-Strauss, C. *The Symmetries of Things*; A K Peters: Natick, MA, USA, 2008;
3. Senechal, M. *Quasicrystals and Geometry*; Cambridge University Press: Cambridge, UK, 1995;
4. Ramsey, F.P. On a Problem of Formal Logic. *Proc. London Math. Soc.* **1930**, *s2-30*, 264–286, doi:10.1112/plms/s2-30.1.264.
5. Graham, R.L.; Rothschild, B.L.; Spencer, J.H. *Ramsey Theory*; 2nd ed.; Wiley: New York, NY, USA, 1990;
6. Diestel, R. *Graph Theory*; 5th ed.; Springer: Berlin/Heidelberg, Germany, 2017;
7. Turán, P. On an Extremal Problem in Graph Theory. *Mat. Fiz. Lapok* **1941**, *48*, 436–452.
8. Mantel, W. Problem 28. *Wiskd. Opgaven* **1907**, *10*, 60–61.
9. Bollobás, B. *Modern Graph Theory*; Springer: New York, NY, USA, 1998;
10. Godsil, C.; Royle, G. *Algebraic Graph Theory*; Springer: New York, NY, USA, 2001;
11. Stanley, R.P. *Enumerative Combinatorics, Vol. 1*; 2nd ed.; Cambridge University Press: Cambridge, UK, 2011;
12. Thäle, C.; Weiß, V. The Combinatorial Structure of Spatial STIT Tessellations. *Discret. Comput. Geom.* **2013**, *50*, 649–672, doi:10.1007/s00454-013-9524-y.
13. Frank, N.P. Detecting Combinatorial Hierarchy in Tilings Using Derived Voronoi Tessellations. *Discret. Comput. Geom.* **2003**, *29*, 459–467, doi:10.1007/s00454-002-0758-3.
14. Calka, P. Precise Formulae for the Distributions of the Numbers of Edges of the Typical Poisson–Voronoi Cell. *Adv. Appl. Probab.* **2003**, *35*, 551–562, doi:10.1239/aap/1059486821.
15. Møller, J. *Lectures on Random Voronoi Tessellations*; Springer: New York, NY, USA, 1994;
16. Cowan, R. Properties of Poisson–Voronoi Tessellations Relevant to Random Spatial Division. In *Statistics of Spatial Processes*; Springer: Berlin/Heidelberg, Germany, 1991; pp. 145–161.
17. Coxeter, H.S.M. *Introduction to Geometry*; 2nd ed.; Wiley: New York, NY, USA, 1969.
18. Gilevich, A.; Shoval, S.; Nosonovsky, M.; Frenkel, V.; Bormashenko, E. Converting Tessellations into Graphs: From Voronoi Tessellations to Complete Graphs. *Mathematics* **2024**, *12*, 2426, doi:10.3390/math12152426.

 doi:10.20944/preprints202606.0392.v1

19. Legchenkova, I.; Frenkel, V.; Shvalb, N.; Shoval, S.; Bormashenko, E. From Chaos to Ordering: New Studies in the Shannon Entropy of 2D Patterns. *Entropy* **2022**, *24*, 802, doi:10.3390/e24060802.
20. Frenkel, V.; Legchenkova, I.; Bormashenko, E.; Shoval, S.; Nosonovsky, V. Extreme Values and Convergence of the Voronoi Entropy for 2D Random Point Processes and for Long-Range Order. *Entropy* **2026**, *28*, 95, doi:10.3390/e28010095.
21. Okabe, A.; Boots, B.; Sugihara, K.; Chiu, S.N. *Spatial Tessellations: Concepts and Applications of Voronoi Diagrams*; 2nd ed.; Wiley: Chichester, UK, 2000.
22. Aurenhammer, F. Voronoi Diagrams---A Survey of a Fundamental Geometric Data Structure. *ACM Comput. Surv.* **1991**, *23*, 345–405, doi:10.1145/116873.116880.
23. Biggs, N. *Algebraic Graph Theory*; 2nd ed.; Cambridge University Press: Cambridge, UK, 1993.
24. Harary, F. *Graph Theory*; Addison-Wesley: Reading, MA, USA, 1969.
25. Wilson, R.J. *Introduction to Graph Theory*; 5th ed.; Pearson Education: Harlow, UK, 2010;
26. Erdos, P.; Stone, A.H. On the Structure of Linear Graphs. *Bull. Am. Math. Soc.* **1946**, *52*, 1087–1091, doi:10.1090/S0002-9904-1946-08715-0.
27. Weisstein, E.W. Cairo Tessellation Available online: https://mathworld.wolfram.com/CairoTessellation.html (accessed on 28 May 2026).
28. Grünbaum, B.; Shephard, G.C. Tilings by Regular Polygons. *Math. Mag.* **1977**, *50*, 227–247, doi:10.2307/2689529.
29. Shi, L.; Xiong, Z.; Wang, H. Quasicrystal Approximants in Isoreticular Metal-Organic Frameworks via Cairo Pentagonal Tiling. *Chem* **2024**, *10*, 2464–2472.
30. Kovács, G.; Nagy, B.; Turgay, N.D. Distance on the Cairo Pattern. *Pattern Recognit. Lett.* **2021**, *145*, 141–146, doi:10.1016/j.patrec.2021.02.002.
31. Erdos, P.; Rényi, A. On Random Graphs I. *Publ. Math. Debrecen* **1959**, *6*, 290–297.
32. Jungck, J. R.; Biswas, P. Graph Theoretic Analyses of Tessellations of Five Aperiodic Polykite Unitiles, *Mathematics* **2025**, *13*(18), 2982; https://doi.org/10.3390/math13182982
33. Alexandrov, A.D. *Convex Polyhedra*; Springer: Berlin/Heidelberg, Germany, 2005;